IEEE Access
Multidisciplinary | Rapid Review | Open Access Journal

Received June 7, 2020, accepted June 11, 2020, date of publication June 16, 2020, date of current version June 30, 2020.

Digital Object Identifier 10.1109/ACCESS.2020.3002920

Coordinated Beamforming for Multi-Cell Non-Orthogonal Multiple Access-Based Spatial Modulation

DENNY KUSUMA HENDRANINGRAT[1], (Member, IEEE), GANDEVA BAYU SATRYA[2], (Senior Member, IEEE), AND I NYOMAN APRAZ RAMATRYANA[3]

[1]Deputy for Standards Development, National Standardization Agency of Indonesia, Jakarta 10340, Indonesia
[2]School of Applied Science, Telkom University, Bandung 40257, Indonesia
[3]Department of IT Convergence Engineering, Kumoh National Institute of Technology, Gumi 39177, South Korea

Corresponding author: Denny Kusuma Hendraningrat (dennykh@ieee.org)

This work was supported by the Directorate of Research and Community Service, Telkom University.

ABSTRACT This paper proposes coordinated beamforming (CB) that works over non-orthogonal multiple access (NOMA) scheme integrated with spatial modulation (SM), termed as CB NOMA-SM, to improve capacity and user fairness. User capacity, ergodic sum capacity (ESC), and user fairness of K number of coordinated base stations (BSs) are simulated and analyzed by comparing them with joint transmission coordinated multi-point based NOMA with SM (JT-CoMP NOMA-SM), NOMA, and orthogonal multiple access (OMA). The results show that the proposed system outperforms the other schemes both in ESC and user fairness due to the enhancing CEU while CCU capacity still can be maintained.

INDEX TERMS Non-orthogonal multiple access (NOMA), coordinated beamforming (CB), spatial modulation (SM), capacity, user fairness.

I. INTRODUCTION

Non-orthogonal multiple access (NOMA) is one of multiple access candidates in next-generation wireless communications, which provides higher spectral efficiency than orthogonal multiple access (OMA) [1], [2]. NOMA multiplexes users superimposed in the power domain over a particular resource [3]–[5]. In downlink NOMA, a base station (BS) allocates less power to cell center user (CCU) than those allocated to cell center user (CEU). In addition, CCU decodes its own signal by removing CEU signal using successive interference cancellation (SIC) [4]–[8].

In multi-cell scenarios, several inter-cell interference (ICI) avoidance techniques have been proposed to improve user performance [9], [10]. In conventional coordinated multi-point (CoMP), a CEU located in overlapping cell area is transmitted by multiple coordinated BSs [11]–[15]. The same resources are allocated to the CEU, then CCU uses SIC to remove ICI caused by CEU signal while receiving signals from multiple CoMP BSs. Therefore, CoMP can enhance data rate in a multi-cell network. However, most of the conventional CoMP only considers single CEU within multiple CoMP BSs [13]–[15]. Considering the number of CEU that may be equal to or more/less than CCUs in practice, joint transmission CoMP with virtual user pairing-based NOMA (JT-CoMP VP-NOMA) [16] and joint transmission CoMP works over NOMA integrated with spatial modulation (JT-CoMP NOMA-SM) [17] are proposed to handle multiple CEUs as well as the ICI issue. In JT-CoMP NOMA-SM, spatial modulation (SM) is used for serving multiple CEUs which are considered ineffective to be transmitted using CoMP technique [18], [19]. Utilizing SM is considered effective to improve capacity in multi-cell scenarios because it can avoid ICI [20]. Based on the evaluation of JT-CoMP NOMA-SM, a CoMP user gets high data rate because it gets signals from multiple coordinated BSs. Assuming there are K number of coordinated BSs within N number of cells and the number of SM antenna is fixed, a fairness problem occurs when the number of coordinated BS is increased. CoMP user capacity increases whereas

The associate editor coordinating the review of this manuscript and approving it for publication was Amjad Mehmood.

SM users capacity depends on the number of antennas used in the BS.

Antenna's beamforming which is coordinated to each other, or known as coordinated beamforming (CB), could be used for overcoming the ICI issue [21]–[24]. In CB based NOMA (CB NOMA), data for CEU are allocated to be only independently available at the serving BS. By using interference alignment based coordinated beamforming (IA-CB) method, the BSs coordinate with each other to optimize their beamforming vectors and to enhance their user capacity. The algorithm chooses its transmitted/received beamforming vector, the other are considered as ICI and will be removed [23]–[26]. The CCU that does not apply CB will encounter ICI due to the signals from neighboring cells. Moreover, CB NOMA can improve both capacity and user fairness because two users paired in each cell are served by its BS independently. By considering superiority of SM such as improving capacity, mitigating ICI and handling multiple CEUs [17]–[20], the SM can be implemented in CB NOMA where one transmitting antenna is activated to transmit symbols at a particular time. The practical use of CB NOMA combined with SM (CB NOMA-SM) depends on the system model. Assuming a cell is having the same number of CCU and CEU, then SM should be utilized to improve CEU capacity [27]–[29]. Otherwise, SM can be used for serving users that are considered ineffective when a resource is allocated [30], [31].

By utilizing more than one transmitting antennas, Multiple-Input Single-Output (MISO) or Multiple-Input Multiple-Output (MIMO) system can be used for further improving SM capacity [32], [33]. Generalized SM (GSM) enhances SM capacity by utilizing MISO or MIMO antenna and activating more than one antennas [34]–[37]. Quadrature SM (QSM) extends capacity of GSM by using an extra modulation spatial dimension [38], [39] In addition, sparse code multiple access (SCMA) combined with SM (SM-SCMA) or QSM can also be utilized to handle the increasing number of users [40].

The main contributions of this paper are summarized as follows.

- A novel CB NOMA-SM is proposed to improve both capacity and user fairness. Different from previous works in [21]–[24], this paper exploits CB NOMA integrated with SM in a generalized multi-cell scenario.
- Instead of the probability of error on IQ domain, this paper estimates probability of error on antenna index by using maximum likelihood (ML) detector. It is different from previous work in [17] that assumed user can detect antenna index perfectly.
- This paper provides a closed-form solution for ergodic sum capacity (ESC) of the proposed system, which is derived through a mathematical analysis by considering imperfect SIC and imperfect channel state information (CSI).

The rest of this paper is arranged as follows: Section II explains system model of the proposed system. Section III provides transmission protocol of the proposed system. Section IV conducts performance analysis of the proposed system such as ESC and user fairness while Section V presents the simulation results. Finally, section VI provides conclusion of this paper.

II. SYSTEM MODEL

In this paper, the system is modeled as a generalized multi-cell system with K number of coordinated BSs within N number of neighboring cells. To compare it with previous work in [17], each coordinated cell consists of a BS, one CEU and one CCU as shown in Fig. 1. The distances from BS to CCU and to CEU are defined as r_{ij} and r_{ik}, respectively. In this case, $i \in 1, 2, \ldots, N$ indicates the i^{th} BS, $j \in 1, 2, \ldots, K$ denotes the j^{th} CCU, and $k \in 1, 2, \ldots, K$ represents the k^{th} CEU. This paper generates user positions by using random user algorithm. The cell radius is assumed as $R = 1$ for normalization. The distance between BSs is assumed as $2R$. In addition, the height of BS antenna is assumed to be $0.01R$. The distances from the j^{th} CCU and the k^{th} CEU to the ith BS antenna, represented by d_{ij} and d_{ik} respectively, can be calculated by using the concepts of trigonometry.

For simplicity, this paper assumes each user has a single antenna and each BS has two antennas ($T_{X_i} = 2$), where T_{X_i} indicates the number of the i^{th} transmitter antenna. In SM system, each BS antenna is combined with IQ domain as an additional information [34]–[37]. Assuming each coordinated cell contains two users, the additional information from SM can be utilized to escalate CEU capacity. Otherwise, SM should be utilized to serve users considered inefficient to be handled by using NOMA.

In practices, users may not be able to perfectly estimate information modulated through antenna index. It can decrease user's capacity, which is represented by a probability of error (PE). This paper denotes PE_{sym} as probability of error caused to error of binary phase-shift keying (BPSK), and PE_{ant} as probability of error that occurs because user cannot detect antenna index perfectly [41], [42].

III. TRANSMISSION PROTOCOL

In this paper, total bandwidth and total power in a cell are normalized by $B = 1$ and $P = 1$, respectively. If α is denoted as power allocation factor for CCU, then $P_j = \alpha P$ and $P_k = \beta P$ can be denoted as power allocation for CCU and CEU, respectively. α is assumed to be 0.1, whereas β can be assigned by 1-α. Fig 2 shows the illustration of the simulated and analyzed scenarios.

For simplicity, this paper assumes that the links between BS antenna and users are identical. Imperfect CSI is considered to have channel estimation error (CSE) because in reality there is no perfect channel estimation [15], [17]. The CSE for the j^{th} CCU and the k^{th} CEU can be modeled by $h_{\varepsilon ij} = h_{ij} - \hat{h}_{ij}$ and $h_{\varepsilon ik} = h_{ik} - \hat{h}_{ik}$, respectively. It assumes that it signal propagates through *Rayleigh Flat Fading* channel independently, channel coefficients are represented by $h_{\varepsilon ij} \sim CN\left(0, \sigma_{\varepsilon ij}\right)$ for the j^{th} CCU, and $h_{\varepsilon ik} \sim CN\left(0, \sigma_{\varepsilon ik}\right)$

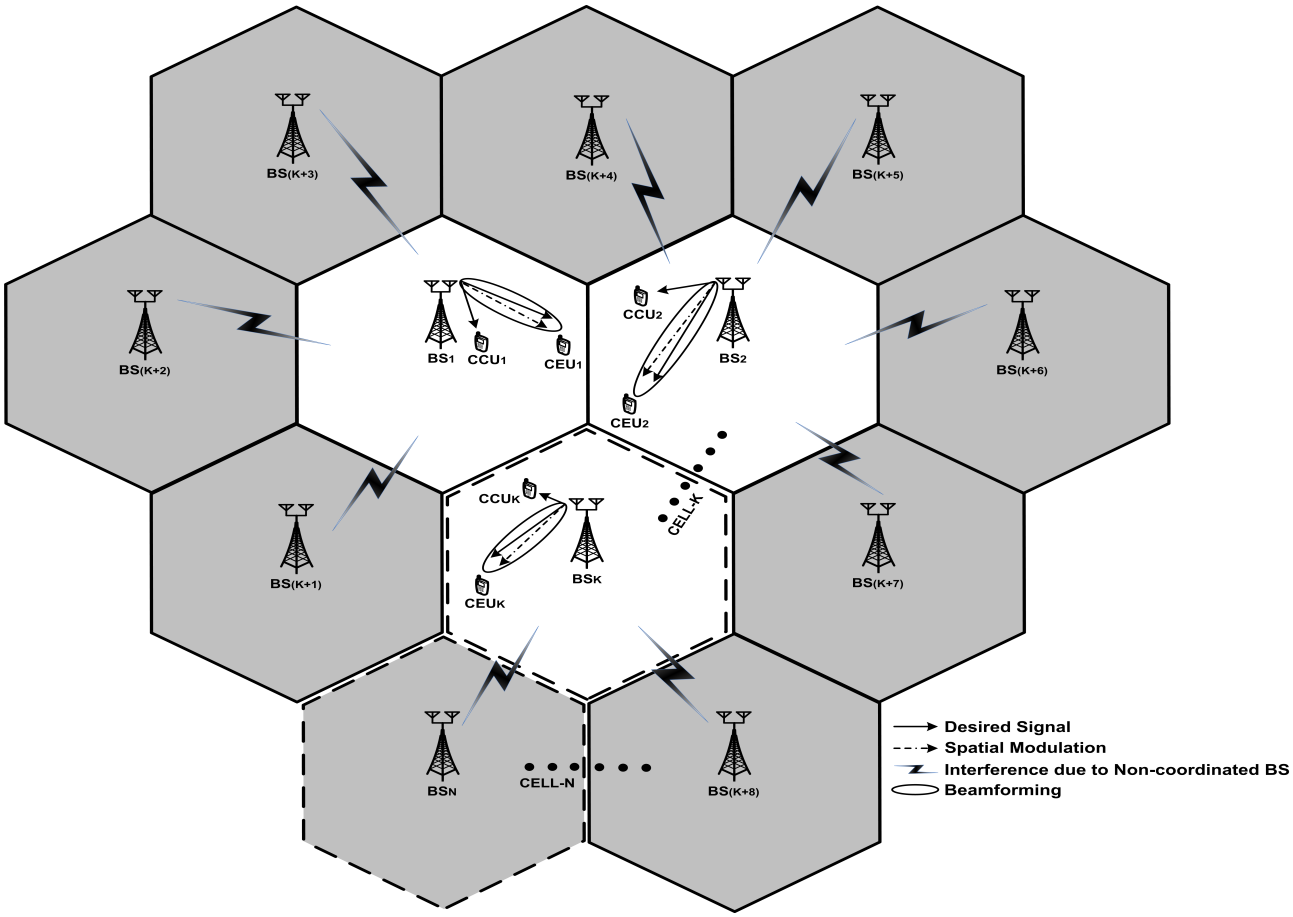

FIGURE 1. Generalized multi-cell systems of the proposed CB NOMA-SM.

for the k^{th} CEU. The received signals of CEU and CCU need to estimate channel gain $|\hat{h}_{ik}|^2$ and $|\hat{h}_{ij}|^2$, respectively. The channel estimation characteristic for CCU is distributed independently with mean zero and can be modeled as $\hat{h}_{ij} \sim CN(0, \hat{\sigma}_{ij} = d_{ij}^{-v} - \sigma_{\varepsilon ij})$. Similarly, the channel estimation characteristic for CEU is modeled as $\hat{h}_{ik} \sim CN(0, \hat{\sigma}_{ik} = d_{ik}^{-v} - \sigma_{\varepsilon ik})$. In this case, $\hat{\sigma}_{ij}$ and $\hat{\sigma}_{ik}$ signifies the estimation variance of link from the i^{th} BS to the j^{th} CCU and to the k^{th} CEU, respectively. While, v denotes path-loss exponent. In this paper, $\sigma_{\varepsilon_{i,j}}$and $\sigma_{\varepsilon_{i,k}}$, assigned as variances of channel estimation error for CCU and CEU from the i^{th} BS, are assumed to be fixed for each channel which is 0.01 [15], [17]. On the other hand, imperfect SIC caused by CCU cannot decode its own message perfectly and assumed to be -25 dB [15], [17].

For i^{th} BS, the superposition code is applied by using the following NOMA scheme.

$$x_i = \sqrt{\alpha P} S_j + \sqrt{\beta P} S_k, \tag{1}$$

where S_j and S_k represent the desired signal for the j^{th} CCU and the k^{th} CEU from the i^{th} BS, respectively.

From CCU's point of view, the total received signals from the i^{th} BS at the j^{th} CCU with given channel estimation error is as follow.

$$\begin{aligned} y_j &= \sum_{i=1}^{N} \left(\hat{h}_{ij} + \sigma_{\varepsilon_{ij}}\right)\left(\sqrt{\alpha P} S_j + \sqrt{\beta P} S_k\right) + n_j \\ &= \hat{h}_{jj}\left(\sqrt{\alpha P} S_j + \sqrt{\beta P} S_k\right) \\ &\quad + \sum_{\substack{i=1 \\ i \neq j}}^{N} \underbrace{\hat{h}_{ij}\left(\sqrt{\alpha P} S_j + \sqrt{\beta P} S_k\right)}_{\text{interference from the other BSs}} \\ &\quad + \sum_{i=1}^{N} \underbrace{\sigma_{\varepsilon_{ij}}\left(\sqrt{\alpha P} S_j + \sqrt{\beta P} S_k\right)}_{\text{channel estimation error}} + n_j, \end{aligned} \tag{2}$$

where n_j represents the noise received by the j^{th} CCU during transmission. The j^{th} CCU decodes its own signal from the i^{th} BS by cancelling the k^{th} CEU signal using SIC, where $i = j = k$. Then, the received SINR at the j^{th} CCU after SIC process is expressed as

$$\tau_j = \frac{\alpha P |\hat{h}_{jj}|^2}{(\alpha + \beta) P \sum\limits_{\substack{i=1 \\ i \neq j}}^{N} |\hat{h}_{ij}|^2 + (\alpha + \beta) P \sum\limits_{i=1}^{N} \sigma_{\varepsilon_{ij}} + N_o}, \tag{3}$$

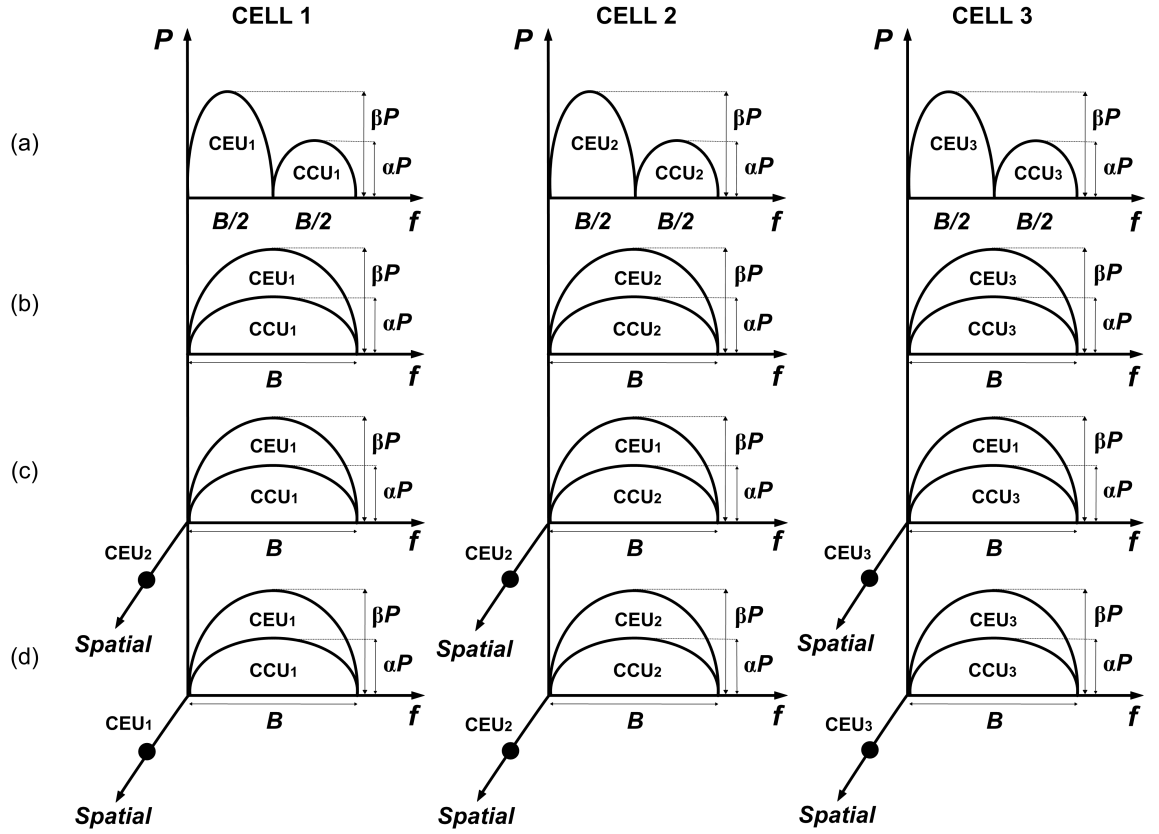

FIGURE 2. Considered scenarios: (a) OMA, (b) NOMA, (c) JT-CoMP NOMA-SM, and (d) CB NOMA-SM.

where N_o represents the additive white Gaussian noise (AWGN). With K number of coordinated BSs within N number of cells, the CEU signals from coordinated BSs can be avoided by coordinating its beamforming. However, CCU still endures ICI that comes from the CCU signals. CCU also suffers ICI from other BSs that do not apply CB. Considering $\alpha + \beta = 1$, the received SINR at the j^{th} CCU when CB is applied can be expressed as follow.

$$\tau_j = \frac{\alpha P|\hat{h}_{jj}|^2}{\alpha P \sum\limits_{\substack{i=1 \\ i\neq j}}^{K} |\hat{h}_{ij}|^2 + P \sum\limits_{i=K+1}^{N} |\hat{h}_{ij}|^2 + P \sum\limits_{i=1}^{N} \sigma_{\varepsilon_{ij}} + N_o}. \quad (4)$$

On the other hand, the total received signal of the k^{th} CEU is given as

$$y_k = \sum_{i=1}^{N} \left(\hat{h}_{ik} + \sigma_{\varepsilon_{ik}}\right) \left(\sqrt{\alpha P} S_j + \sqrt{\beta P} S_k\right) + n_k, \quad (5)$$

where n_k is a noise received by the k^{th} CEU during transmission. Similarly, the CEU signals from coordinated BSs can be avoided because the beamforming vector can be chosen by coordinating its beamforming. In addition, IA-CB removes other signals from the coordinated BSs. However, CEU still suffers ICI from other BSs that do not apply CB. So, the received SINR at the k^{th} CEU can be written as follow.

$$\tau_k = \frac{\beta P|\hat{h}_{kk}|^2}{\alpha P|\hat{h}_{kk}|^2 + P \sum\limits_{i=K+1}^{N} |\hat{h}_{ik}|^2 + P \sum\limits_{i=1}^{N} \sigma_{\varepsilon_{ik}} + N_o}. \quad (6)$$

IV. PERFORMANCE ANALYSIS

A. ERGODIC SUM CAPACITY

In this section, ESC of the proposed system is determined for users located in K number of coordinated BSs within N number of cells. By considering $\rho = P/N_o$, then SINR of the j^{th} CCU in equation (4) is addressed as follow

$$\tau_j = \frac{\alpha\rho|\hat{h}_{jj}|^2}{\alpha\rho \sum\limits_{\substack{i=1 \\ i\neq j}}^{K} |\hat{h}_{ij}|^2 + \rho \sum\limits_{i=K+1}^{N} |\hat{h}_{ij}|^2 + \rho \sum\limits_{i=1}^{N} \sigma_{\varepsilon_{ij}} + 1}. \quad (7)$$

The imperfect SIC should be considered when user cannot estimate its channel and CCU cannot decode its signal perfectly [15], [17]. Then, equation (7) can be derived as follow.

$$\tau_j = \frac{\alpha\rho|\hat{h}_{jj}|^2}{\underbrace{\alpha\rho \sum\limits_{\substack{i=1 \\ i\neq j}}^{K} |\hat{h}_{ij}|^2}_{ICI\ CB} + \underbrace{\rho \sum\limits_{i=K+1}^{N} |\hat{h}_{ij}|^2}_{ICI\ non-CB} + \underbrace{\rho \sum\limits_{i=1}^{N} \sigma_{\varepsilon_{ij}}}_{im\ CSI} + \underbrace{\rho\gamma}_{im\ SIC} + 1}, \quad (8)$$

where γ represents residual interference caused by CEU signal that may not be canceled perfectly at CCU. Considering that CCU located in the coordinated BSs does not apply CB, the ICI CB happens due to power allocation to CCU from the neighboring cells. It can be ignored because the ICI is assumed to be very small. Therefore, the ICI CB on equation (8) can be deleted. The ICI non-CB represents ICI caused by BSs that do not apply CB.

Assuming that each beam is coordinated perfectly as has been derived in equation (6), CEU suffers inter-NOMA interference (INI) as well as ICI non-CB. Then, SINR of the k^{th} CEU can be calculated as:

$$\tau_k = \frac{\beta\rho|\hat{h}_{kk}|^2}{\underbrace{\alpha\rho|\hat{h}_{kk}|^2}_{INI} + \underbrace{\rho\sum_{i=K+1}^{N}|\hat{h}_{ik}|^2}_{ICI\ non-CB} + \underbrace{\rho\sum_{i=1}^{N}\sigma_{\varepsilon_{ik}}}_{im\ CSI} + 1}. \quad (9)$$

The achievable throughput for the j^{th} CCU and the k^{th} CEU in the i^{th} cell can be written as below.

$$C_j = log_2\left(1+\tau_j\right), \quad (10)$$

$$C_k = log_2\left(1+\tau_k\right). \quad (11)$$

In the proposed system, CEU utilizes SM to further improve its capacity because the number of CCU is equal to the number of CEU, as explained in Section II. Due to the inability of user in detecting both IQ and antenna index perfectly, the CEU capacity combined with CB NOMA and SM can be written as

$$C_k = log_2\left(1+\tau_k\right) + (1-PE_{sym,k})log_2(M) + (1-PE_{ant,k})\left\lfloor log_2\binom{T_{X_i}}{T_{A_i}}\right\rfloor, \quad i=k. \quad (12)$$

In this paper, M represents the M-ary of modulation constellation order. While, T_{A_k} represents the number of active antennas in the i^{th} BS. As a note, SM could be added to support CCU capacity if needed. Therefore, the achievable sum rate of the proposed system in the i^{th} cell is given as below.

$$C_i^{erg} = C_j + C_k, \quad i=j=k. \quad (13)$$

Moreover, ESC of the proposed system with K number of coordinated BSs within N number of cells can be calculated as:

$$C_{total}^{erg} = \sum_{i=1}^{K} C_i^{erg}, \quad (14)$$

Given the probability density function (PDF) in [15], the exact CCU capacity on equation (10) can be calculated by solving the equation below.

$$C_j^{\text{exact}} = E\{C_j\} = \int_0^\infty \log_2\left(x+a\right) f_{X_j}(x)dx - \int_0^\infty \log_2\left(y+a\right) f_{Y_j}(y)dy, \quad (15)$$

where E represents expectation operator, and $a = \rho\sum_{i=1}^{N}\sigma_{\varepsilon_{ij}} + \rho\gamma + 1$.

First, let suppose $X_j \triangleq \alpha\rho\sum_{i=1}^{N}|\hat{h}_{ij}|^2$ and $Y_j \triangleq \alpha\rho\sum_{i=1,i\neq j}^{N}|\hat{h}_{ij}|^2$. The PDF of X_j can be determined through exponential random variables (RVs) of total N number of cells whereas $N-1$ should be considered for Y_j. The parameters of exponential RVs are assumed to be different because the distance from each i^{th} BS to the j^{th} CCU is different. It makes the channel gain variance is also different for each $\hat{h}_{ij}$. The PDF of each exponential RV can be expressed as follow.

$$f_{X_{ij}}(x) = \frac{d(F_{X_{ij}}(x))}{dx} = \frac{d(1-\exp(-w_{ij}x))}{dx} = w_{ij}\exp(-w_{ij}x), \quad (16)$$

$$f_{Y_{ij}}(y) = \frac{d(F_{Y_{ij}}(y))}{dy} = \frac{d(1-\exp(-w_{ij}y))}{dy} = w_{ij}\exp(-w_{ij}y), \quad (17)$$

where, w_{ij} represents each parameter of exponential RVs. By using sum exponential, the PDF of X_j and Y_j can be derived as:

$$f_{X_j}(x) = \sum_{i=1}^{N} f_{X_{ij}}(x) = \sum_{i=1}^{N} f_{X_{ij}}(x)\prod_{\substack{h=1\\h\neq i}}^{N}\frac{w_{hj}}{w_{hj}-w_{ij}}, \quad N\geq 2. \quad (18)$$

$$f_{Y_j}(y) = \sum_{i=1}^{N} f_{Y_{ij}}(y), \quad i\neq j, = \sum_{\substack{i=1\\i\neq j}}^{N} f_{Y_{ij}}(y)\prod_{\substack{h=1\\h\neq i\\h\neq j}}^{N}\frac{w_{hj}}{w_{hj}-w_{ij}}, \quad N\geq 3. \quad (19)$$

By inserting equation (16) into equation (18) and equation (17) into equation (19), the CCU capacity for the proposed system can be solved by using PDF of $f_{X_j}(x)$ and $f_{Y_j}(y)$. Therefore, C_j^{exact} of can be written as

$$C_j^{exact} = \frac{1}{\ln(2)}\left\{\sum_{i=1}^{K}\left(\ln(a) - \exp(aw_{ij})\text{Ei}(-aw_{ij})\right)\right\} \times \prod_{\substack{h=1\\h\neq i}}^{N}\frac{w_{hj}}{w_{hj}-w_{ij}}$$

$$-\sum_{\substack{i=1\\ i\neq j}}^{K}\left(\ln(a)-\exp(aw_{ij})\mathrm{Ei}(-aw_{ij})\right)\times\prod_{\substack{h=1\\ h\neq i\\ h\neq j}}^{N}\frac{w_{hj}}{w_{hj}-w_{ij}}\Bigg\}, \quad (20)$$

where $w_{ij}=\frac{1}{\alpha\rho\hat{\sigma}_{ij}}$ for $1\leq i\leq K$, and $w_{ij}=\frac{1}{\rho\hat{\sigma}_{hj}}$ for $K+1\leq i\leq N$. Here, $\hat{\sigma}_{ij}$ denotes the mean of the i^{th} exponential RVs of X_j and Y_j.

Similarly, given $PE^{exact}_{sym,k}$ as stated in Appendix A.1 and $PE^{exact}_{ant,k}$ stated in Appendix A.2, then the exact CEU capacity on equation (12) can be calculated as follow.

$$C_k^{\text{exact}}=\int_0^{\infty}\log_2(x+b)f_{X_k}(x)dx+(1-PE^{exact}_{sym,k})log_2(M)+(1-PE^{exact}_{ant,k})\left\lfloor log_2\binom{T_{X_i}}{T_{A_i}}\right\rfloor,\quad i=k, \quad (21)$$

where $b=\rho\sum_{i=1}^{N}\sigma_{\varepsilon_{ik}}+1$. The PDF of $f_{X_k}(x)$ can be derived as

$$f_{X_{ik}}(x)=\frac{F_{X_{ik}(x)}}{dx}=\frac{d(1-\exp(-l_{ik}x))}{dx}=l_{ik}\exp(-l_{ik}x). \quad (22)$$

Therefore, by substituting equation (22) into equation (21), C_k^{exact} is given as

$$\begin{aligned}C_k^{\text{exact}}&=\int_0^{\infty}\log_2(x+b)\,l_{ik}\exp(-l_{ik}x)(x)dx\\&\quad+(1-PE^{exact}_{sym,k})log_2(M)\\&\quad+(1-PE^{exact}_{ant,k})\left\lfloor log_2\binom{T_{X_i}}{T_{A_i}}\right\rfloor\\&=\frac{1}{\ln(2)}\{\ln(b)-\exp(bl_{ik})\mathrm{Ei}(-bl_{ik})\}\\&\quad+(1-PE^{exact}_{sym,k})log_2(M)\\&\quad+(1-PE^{exact}_{ant,k})\left\lfloor log_2\binom{T_{X_i}}{T_{A_i}}\right\rfloor,\quad i=k,\end{aligned} \quad (23)$$

where $l_{ik}=\frac{1}{\rho\hat{\sigma}_{ik}}$.

Furthermore, the exact achievable sum rate of the proposed system in i^{th} cell can be calculated by substituting both equation (20) and equation (23) into equation (13). Therefore, the exact ESC of the proposed system with K number of coordinated BSs within N number of cells can be written as follow.

$$C_{total}^{exact}=\sum_{i=1}^{K}C_i^{exact}. \quad (24)$$

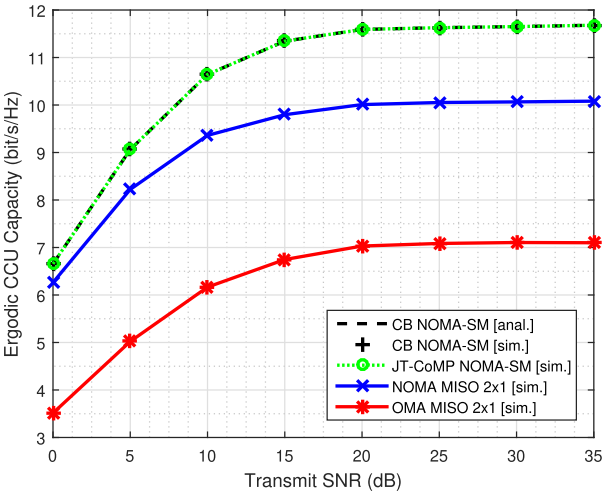

FIGURE 3. Ergodic CCU capacity.

B. USER FAIRNESS

In this section, user fairness is determined based on the achievable data rate for each user. In [43], Jain's fairness is addressed as a method to analyze user fairness. It physically presents the deviation of user throughput in an observed area. Fairness index for all users distributed in K number of coordinated BSs within N number of cells can be measured as below.

$$FI=\frac{\left(\sum_{j=1}^{K}C_j+\sum_{k=1}^{K}C_k\right)^2}{U\left[\sum_{j=1}^{K}(C_j)^2+\sum_{k=1}^{K}(C_k)^2\right]}, \quad (25)$$

where U represents total number of users located in K number of coordinated cells.

V. SIMULATION RESULT

In this section, ESC and user fairness of the proposed CB NOMA-SM are analyzed and compared with JT-CoMP NOMA-SM, NOMA, and OMA. CB NOMA is also considered as a part of the proposed system without the use of SM technique. In other words, this paper uses three coordinated BSs ($K=3$) within twelve cell models ($N=12$) to be simulated and analyzed.

Fig. 3 shows that the proposed system has 64.84% and 15.78% better CCU capacity at $\rho=20$ dB than OMA and NOMA, respectively. While being compared to JT-CoMP NOMA-SM, the proposed system has the same CCU capacity because the CCU that does not apply CB technique suffers ICI from the neighboring BSs. So, both comparison schemes have the same ICI pattern as JT-CoMP NOMA-SM due to the power allocated to CCU from the neighboring BS.

In Fig. 4, the proposed system has 302.7%, 165.1%, and 73.2% higher CEU capacity at $\rho=20$ dB than OMA, NOMA, and JT-CoMP NOMA-SM, respectively. It occurs because the proposed system utilizes both CB and SM

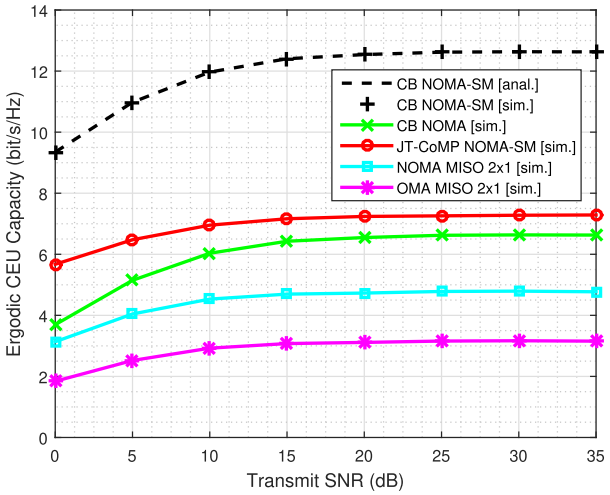

FIGURE 4. Ergodic CEU capacity.

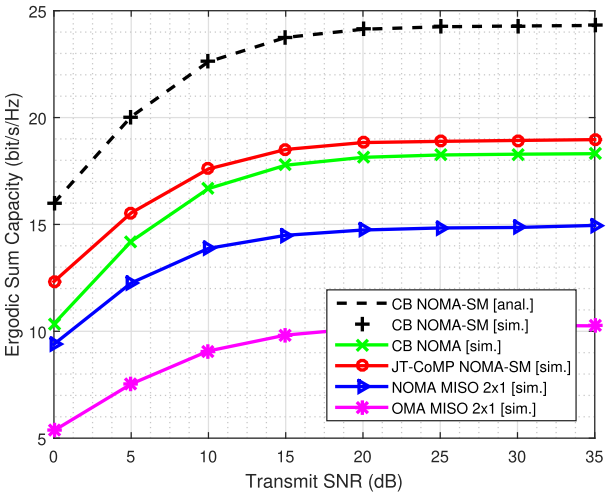

FIGURE 5. Ergodic sum capaicity (ESC).

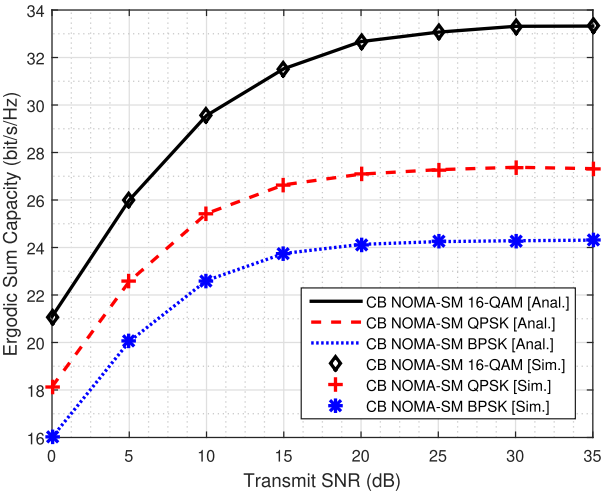

FIGURE 6. The effect of different modulation of the proposed system on the ESC.

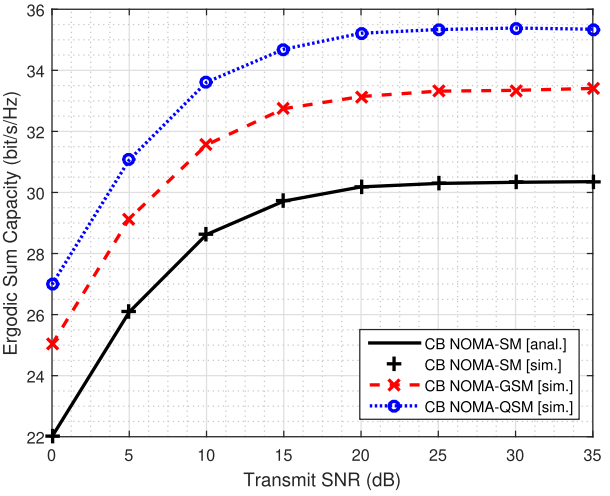

FIGURE 7. The effect of the number of BS antennas on the proposed system.

techniques over NOMA scheme to optimize the power and bandwidth to CEU while JT-CoMP NOMA-SM divides its CEUs into a CoMP user and SM users to be served separately. For $\rho = 20$ dB, CB NOMA has 92.75% lower CEU capacity than CB NOMA-SM. By using BPSK, SM can improve approximately 2 bit/s/Hz/cell higher CEU capacity than those without SM at $\rho = 20$ dB. It proves that SM can be utilized to improve CEU capacity.

Fig. 5 shows that ESC of the proposed system outperforms both JT-CoMP NOMA-SM and CB NOMA. The proposed system has 137.96%, 63.7%, and 28.14% higher ESC at $\rho = 20$ dB than OMA, NOMA, and JT-CoMP NOMA-SM, respectively. Without utilizing SM, CB NOMA has 3.66% and 24.82% lower ESC at $\rho = 20$ dB than JT-CoMP NOMA-SM and CB NOMA-SM, respectively. Based on Fig. 3 and Fig. 4, it is clear that ESC of the proposed system increases because of the enhancing CEU capacity.

Fig. 6 shows that increasing modulation order can improve ESC. The proposed system that uses 16-QAM has 35.39% and 20.59% higher ESC at $\rho = 20$ dB than BPSK and QPSK, respectively. It is because the modulation order improves the combinations of index modulation.

Fig. 7 shows that ESC of CB NOMA-SM can be improved by utilizing GSM or QSM. By considering $T_{X_i} = 8$, ESC of CB-NOMA SM improves 9.8% and 16.7% at $\rho = 20$ dB, when GSM and QSM are applied, respectively. By activating two transmitting antennas as its index ($T_{A_i} = 2$), GSM can improve SM index due to the increasing antenna combinations. While QSM escalates capacity of SM index by combining antenna index with modulation spatial dimension.

Moreover, user fairness of the proposed system outperforms other schemes as shown in Fig. 8. At $\rho = 20$ dB, the proposed system has 21.78%, 20.37%, 7.82%, and 11.89% higher fairness index than OMA, NOMA, JT-CoMP NOMA-SM, and CB NOMA, respectively. It is caused by

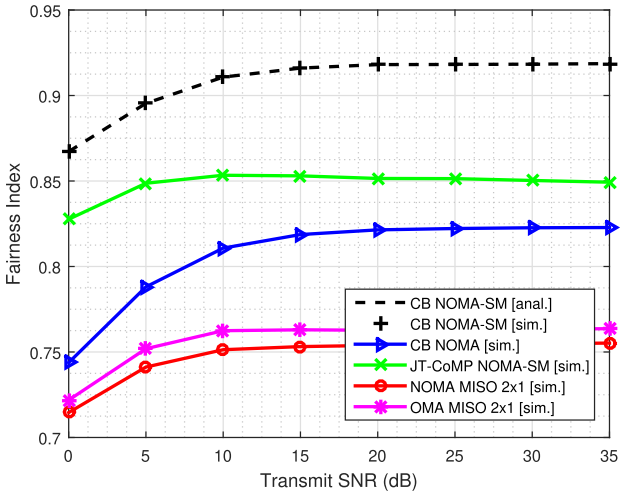

FIGURE 8. User fairness.

the increasing of CEU capacity of the proposed system to be closer to the CCU capacity, due to the combination of both CB and SM techniques. In addition, the fairness index of JT-CoMP NOMA-SM decreases when transmitted SNR is increased. It happens because CoMP user capacity increases if transmitted SNR is increased, whereas SM user's capacity depends on SM antenna used.

VI. CONCLUSION

This paper proposes a novel CB NOMA-SM to enhance capacity and user fairness. The simulation results show that the proposed system has the same CCU capacity compared to JT-CoMP NOMA-SM. In $\rho = 20$ dB, the proposed system has 302.7%, 165.1%, and 73.2% higher CEU capacity than OMA, NOMA, and JT-CoMP NOMA-SM, respectively. Furthermore, ESC of the proposed system has 137.96%, 63.7%, and 28.14% higher ESC at $\rho = 20$ dB than OMA, NOMA, and JT-CoMP NOMA-SM, respectively. Increasing modulation order can improve ESC. Capacity of CB NOMA-SM can be improved by utilizing GSM or QSM. In addition, it also has 21.78%, 20.37%, 7.82%, and 11.89% higher fairness index than OMA, NOMA, JT-CoMPNOMA-SM, and CB NOMA, respectively. Moreover, both ESC and user fairness of the proposed system outperforms other schemes due to the enhancing CEU capacity, while the CCU capacity can be maintained.

For future work, a different method of index modulation technique can be exploited to achieve higher spectral efficiency.

APPENDIX

A.1. DERIVATION PROBABILITY OF ERROR FOR SYMBOL DETECTION

This section derives PE_{sym} for CEU located in the K number of coordinated cells. BS is assumed to transmit signal mapped using BPSK symbol. Considering information of NOMA signal in each i^{th} BS is superimposed with power allocation $(\alpha + \beta)P$, the transmitted signal from the i^{th} BS is given as

$$x_i^* = \sqrt{(\alpha+\beta)P}S_k, \quad \text{where } i = k. \tag{26}$$

In this case, x_i^* denotes transmitted signal from the i^{th} BS to CEU. During transmission, CEU receives information transmitted in the imperfect CSI condition [44]. Received signal of the k^{th} CEU for $1 \leq i \leq K$ by considering imperfect CSI is given as

$$y_k^* = \sum_{i=1}^{K} \hat{h}_{ik}\sqrt{P}S_k + \sum_{i=K+1}^{N} \hat{h}_{ik}\left(\sqrt{\alpha P}S_j + \sqrt{\beta P}S_k\right) + \sum_{i=1}^{N}\sqrt{P}\sigma_{\varepsilon_{ik}} + n_k. \tag{27}$$

Considering $\hat{y}_k$ denotes the desired signal at the k^{th} CEU, decoded information of $\hat{y}_k$ may be different with y_k because of error transmission. Considering decoded signal in [42], error symbol detection of the k^{th} CEU for $1 \leq i \leq K$ can be calculated as

$$PE_{sym,k} = \left\lfloor \frac{\hat{y}_k - y_k}{\sqrt{(\alpha+\beta)P}} \right\rfloor. \tag{28}$$

The exact PE_{sym} for the the k^{th} CEU, i.e. $PE_{sym,k}^{exact}$, can be derived by solving

$$\begin{aligned} PE_{sym,k}^{exact} &= [1-\lambda_k]\,\lambda_k \\ &= \left[1 - \frac{1}{\pi}\int_0^{\pi/2} MGF_{\delta_k}\left(\frac{1}{sin^2\theta}\right)d\theta\right] \\ &\quad \times \frac{1}{\pi}\int_0^{\pi/2} MGF_{\delta_k}\left(\frac{1}{sin^2\theta}\right)d\theta, \end{aligned} \tag{29}$$

where δ_k represents SNR of the k^{th} CEU for the different constellation point of BPSK symbol. Furthermore, δ_k can be written as

$$\delta_k = \frac{\rho\left|\hat{h}_{kk}\right|^2}{\rho\sum\limits_{\substack{i=1\\ i\neq k}}^{N}\left|\hat{h}_{ik}\right|^2 + \rho\sum\limits_{i=1}^{N}\sigma_{\varepsilon_{ik}} + 1}. \tag{30}$$

In the case where each random variable is distributed independently through Rayleigh fading channel, PDF of δ_k can be calculated as

$$f_{\delta_k}(\mu_{ik}) = \frac{\left(\frac{\hat{\mu}_{\delta_k}}{\phi_{\delta_k} g_k}\right)}{Q\left(\phi_{\delta_k}, q_k\right)}\left[1 + \frac{\mu_{ik}\hat{\mu}_{\delta_k}}{\phi_{\delta_k} g_k}\right]^{-(\phi_{\delta_k}+q_k)}(\mu_{ik})^{\phi_{\delta_k}-1}, \tag{31}$$

where $i = k$. In this case, Q is a function defined in [45], [46]. In addition, $q_k = 1/g_k$ where g_k is given as

$$g_k = \frac{(\hat{\mu}_{kk})^2}{\left(\phi_{\delta_k} + \sum\limits_{i=3}^{N}\hat{\mu}_{kk}\right)\left(\hat{\mu}_k + \sum\limits_{i=1}^{N}\sigma_{\varepsilon_{ik}} + \frac{1}{\rho}\right)^2}. \tag{32}$$

Here, $\phi_{\delta_k} = 1$ is assumed for all channels and $\hat{\mu}_{ik} = Ei\left(\hat{\sigma}_{ik}\right)$. By using equation (31) and mathematical rearrangement given in [46], λ_k can be obtained as

$$\lambda_k = \frac{2\mho_k z^{5/2}}{3}\left[\frac{\psi_{A_k}}{\Omega_k \delta\left(\phi_{\delta_k}+q_k\right)} + \frac{\psi_{B_k}+\psi_{C_k}}{\delta\left(\phi_{\delta_k}\right)} + \frac{\psi_{D_k}+\psi_{E_k}+\psi_{F_k}}{z/3}\right], \quad (33)$$

where,

$$\mho_k = \frac{\delta\left(\phi_{\delta_k}\right)}{\pi Q\left(\phi_{\delta_k}, q_k\right)}, \quad (34)$$

$$\Omega_k = \frac{g_k}{\hat{\mu}_{\delta_k}/\phi_{\delta_k}}, \quad (35)$$

$$\psi_{A_k} = \delta\left(q_k\right) F_N\left[\left\{-3/2, \phi_{\delta_k}\right\}, \{-1/2, 1-q_k\}, \Omega_k\right], \quad (36)$$

$$\psi_{B_k} = 2\sqrt{\pi}\frac{\delta\left(\phi_{\delta_k}+3/2\right)\delta\left(q_k-3/2\right)}{\delta\left(\phi_{\delta_k}+q_k\right)}, \quad (37)$$

$$\psi_{C_k} = \frac{3\left(\Omega_k\right)^{q_k-3/2}\delta\left(-q_k\right)}{3-2q_k} \times F_N\left[\left\{q_k-3/2, q_k+\phi_{\delta_k}\right\}, \{q_k-1/2, 1+q_k\}, \Omega_k\right], \quad (38)$$

$$\psi_{D_k} = -2\sqrt{\pi}\frac{\delta\left(\phi_{\delta_k}+1/2\right)\delta\left(q_k-1/2\right)}{\delta\left(\phi_{\delta_k}\right)\delta\left(\phi_{\delta_k}+q_k\right)}, \quad (39)$$

$$\psi_{E_k} = \frac{2\delta\left(-q_k\right)}{\sqrt{\Omega_k}\delta\left(\phi_{\delta_k}+q_k\right)} \times F_N\left[\left\{-1/2, \phi_{\delta_k}\right\}, \{-1/2, 1-q_k\}, \Omega_k\right], \quad (40)$$

$$\psi_{F_k} = \frac{2\left(\Omega_k\right)^{q_k-1/2}\delta\left(-q_k\right)}{\left(1-2q_k\right)\delta\left(\phi_{\delta_k}\right)} \times F_N\left[\left\{q_k-1/2, q_k+\phi_{\delta_k}\right\}, \{q_k+1/2, 1+q_k\}, \Omega_k\right]. \quad (41)$$

$$z = \left(2\left\lfloor log_2\left(M\right)\right\rfloor - 1\right)\frac{\pi}{M}. \quad (42)$$

Here, $F_N\left[\{.,.\},\{.,.\}\right]$ is a generalized hyper-geometric function [46]. Therefore, the exact probability of error for the k^{th} CEU where $3 \le i \le K$ in equation (29) can be rewritten as

$$PE_{sym,k}^{exact} = \left[1 - \left(\frac{2\mho_k z^{5/2}}{3}\left[\frac{\psi_{A_k}}{\Omega_k\delta\left(\phi_{\delta_k}+q_k\right)} + \frac{\psi_{B_k}+\psi_{C_k}}{\delta\left(\phi_{\delta_k}\right)} + \frac{\psi_{D_k}+\psi_{E_k}+\psi_{F_k}}{z/3}\right]\right)\right] \times \frac{2\mho_k z^{5/2}}{3}\left[\frac{\psi_{A_k}}{\Omega_k\delta\left(\phi_{\delta_k}+q_k\right)} + \frac{\psi_{B_1}+\psi_{C_k}}{\delta\left(\phi_{\delta_k}\right)} + \frac{\psi_{D_k}+\psi_{E_k}+\psi_{F_k}}{z/3}\right]. \quad (43)$$

Fig. 9 validates the probability of error for symbol detection that has been derived in equation (43).

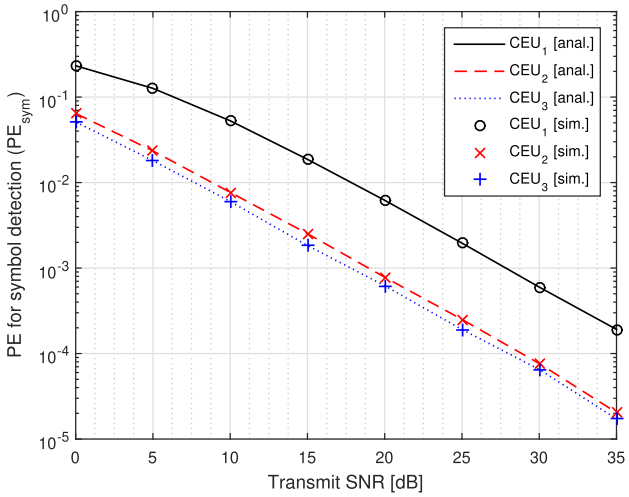

FIGURE 9. Probability of error for symbol detection (PE_{sym}).

A.2 DETERMINING PROBABILITY OF ERROR FOR ML DETECTION

In this case, CEU estimates antenna index by using ML detector. For each k^{th} CEU, ML detection can be derived as

$$\zeta_k = \underset{T_{X_k}}{argmin}\left\|\frac{y_k}{\sum_{\substack{i=1\\i\neq k}}^{N} S_k} - \frac{\sqrt{\rho}\hat{h}_{kk}}{\sqrt{\rho}\sum_{\substack{i=1\\i\neq k}}^{N}\hat{h}_{ik} + \sqrt{\rho}\sum_{i=1}^{N}\sigma_{\varepsilon_{ik}} + 1}\right\|^2, \quad (44)$$

where ζ_k is the detected transmitting antenna set in the k^{th} CEU. Furthermore, performance error of the ML detector can be calculated as

$$PE_{ant,k} \le \frac{1}{N_H log_2\left(N_H\right)}\sum_{p=1}^{N_H}\sum_{\substack{p=1\\p\neq q}}^{N_H} N_{B_{p,q}} Q(A_k), \quad (45)$$

where $N_{B_{p,q}}$ represents the number of error bits between antenna constellation points mapped in p axis and q ordinate. N_H is the power of two of possibility antenna constellation points. For ML detector based GSM method, A_k is derived as

$$A_k = \frac{\sqrt{\bar{\tau}_k}}{T_{A_i}}\left|\sum_{s=1}^{T_{A_i}}\left[\hat{h}_{ik(ps)} - \hat{h}_{ik(qs)}\right]\right|^2, \quad i = k, \quad (46)$$

where $\hat{h}_{ik(ps)}$ and $\hat{h}_{ik(qs)}$ represent channel gain from s^{th} BS antenna in the i^{th} BS to the k^{th} CEU mapped in p axis and q ordinate. The function of $Q(.)$ is derived as

$$Q(.) = \frac{1}{\sqrt{2\pi}}\int_0^{\infty} exp\left(-u^2/2\right) du, \quad (47)$$

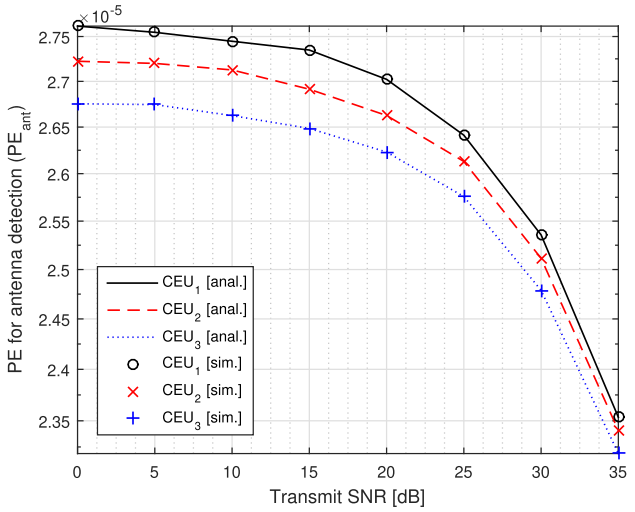

FIGURE 10. **Probability of error for ML detection (PE_{ant}).**

Given the closed-form solution of Q function in [41], [47], then equation (47) can be written as

$$Q(A_k) = (\eta_k)^{T_{A_i}} \sum_{s=1}^{T_{A_i}} \binom{T_{A_i}+s}{s} (1-\eta_k)^s, \quad i = k, \tag{48}$$

where $\eta_k = \frac{1}{2}\left(1 - \sqrt{\frac{\hat{\sigma}_{kk}}{1+\sum_{\substack{i=1\\ i\neq k}}^{N} \hat{\sigma}_{ik} + \sum_{i=1}^{N} \sigma_{\varepsilon_{ik}}}}\right)$. Moreover, exact performance error of ML detector in the k^{th} CEU can be written as

$$PE_{ant,k}^{exact} \leq \frac{1}{N_H log_2(N_H)} \sum_{p=1}^{N_H} \sum_{\substack{p=1\\ p\neq q}}^{N_H} N_{B_{p,q}} Q(A_k). \tag{49}$$

Fig. 10 validates the probability of error for ML detection has been derived in equation (49) by assuming $T_{X_i} = 2$ and $T_{A_i} = 1$ for simplicity.

ACKNOWLEDGEMENT

This research was a collaboration between the National Standardization Agency of Indonesia (BSN), Kumoh National Institute of Technology, and School of Applied Science, Telkom University.

REFERENCES

[1] Z. Ding, X. Lei, G. K. Karagiannidis, R. Schober, J. Yuan, and V. K. Bhargava, "A survey on non-orthogonal multiple access for 5G networks: Research challenges and future trends," *IEEE J. Sel. Areas Commun.*, vol. 35, no. 10, pp. 2181–2195, Oct. 2017.

[2] A. Benjebbour, A. L. K. Saito, Y. Kishiyama, and T. Nakamura, *Signal Process. for 5G: Algorithms Implementations*, 1st ed. Hoboken, NJ, USA: Wiley, 2016.

[3] S. M. R. Islam, N. Avazov, O. A. Dobre, and K.-S. Kwak, "Power-domain non-orthogonal multiple access (NOMA) in 5G systems: Potentials and challenges," *IEEE Commun. Surveys Tuts.*, vol. 19, no. 2, pp. 721–742, 2nd Quart., 2017.

[4] M. B. Shahab, M. F. Kader, and S. Y. Shin, "On the power allocation of non-orthogonal multiple access for 5G wireless networks," in *Proc. Int. Conf. Open Source Syst. Technol. (ICOSST)*, Dec. 2016, pp. 89–94.

[5] Y. Saito, Y. Kishiyama, A. Benjebbour, T. Nakamura, A. Li, and K. Higuchi, "Non-orthogonal multiple access (NOMA) for cellular future radio access," in *Proc. IEEE 77th Veh. Technol. Conf. (VTC Spring)*, Jun. 2013, pp. 1–5.

[6] G. B. Satrya and S. Y. Shin, "Security enhancement to successive interference cancellation algorithm for non-orthogonal multiple access (NOMA)," in *Proc. IEEE 28th Annu. Int. Symp. Pers., Indoor, Mobile Radio Commun. (PIMRC)*, Oct. 2017, pp. 1–5.

[7] G. B. Satrya and S. Y. Shin, "Enhancing security of SIC algorithm on non-orthogonal multiple access (NOMA) based systems," *Phys. Commun.*, vol. 33, pp. 16–25, Apr. 2019.

[8] S. Larasati, I. N. A. Ramatryana, and K. Anwar, "High-rate coded random access for non-orthogonal multiple access with human priority," in *Proc. 2nd Int. Conf. Telematics Future Gener. Netw. (TAFGEN)*, Jul. 2018, pp. 25–30.

[9] A. S. Hamza, S. S. Khalifa, H. S. Hamza, and K. Elsayed, "A survey on inter-cell interference coordination techniques in OFDMA-based cellular networks," *IEEE Commun. Surveys Tuts.*, vol. 15, no. 4, pp. 1642–1670, 4th Quart., 2013.

[10] N. Katiran, N. Fisal, S. K. S. Yusof, S. M. M. Maharum, A. S. A. Ghafar, and F. A. Saparudin, "Inter-cell interference mitigation and coordination in CoMP systems," in *Informatics Engineering and Information Science*. Berlin, Germany: Springer, 2011, pp. 654–665.

[11] M. S. Ali, E. Hossain, and D. I. Kim, "Coordinated multipoint transmission in downlink multi-cell NOMA systems: Models and spectral efficiency performance," *IEEE Wireless Commun.*, vol. 25, no. 2, pp. 24–31, Apr. 2018.

[12] J. Wu, J. Zeng, X. Su, X. Xu, and L. Xiao, "Joint CoMP and power allocation in ultra dense networks," in *Proc. Wireless Telecommun. Symp. (WTS)*, Apr. 2017, pp. 1–5.

[13] J. Choi, "Non-orthogonal multiple access in downlink coordinated two-point systems," *IEEE Commun. Lett.*, vol. 18, no. 2, pp. 313–316, Feb. 2014.

[14] A. Beylerian and T. Ohtsuki, "Coordinated non-orthogonal multiple access (CO-NOMA)," in *Proc. IEEE Global Commun. Conf. (GLOBECOM)*, Dec. 2016, pp. 1–5.

[15] F. W. Murti, R. F. Siregar, and S. Y. Shin, "Exploiting non-orthogonal multiple access in downlink coordinated multipoint transmission with the presence of imperfect channel state information," Dec. 2018, *arXiv:1812.10266*. [Online]. Available: https://arxiv.org/abs/1812.10266

[16] D. K. Hendraningrat, M. B. Shahab, and S. Y. Shin, "Virtual user pairing based nono-rthogonal multiple access in downlink coordinated multipoint transmissions," *IET Commun.*, to be published, doi: 10.1049/iet-com.2019.0955.

[17] D. K. Hendraningrat, B. Narottama, and S. Y. Shin, "Non-orthogonal multiple access in downlink coordinated multipoint transmissions," *Phys. Commun.*, vol. 39, Apr. 2020, Art. no. 101017.

[18] E. Soujeri, *Advanced Index Modulation Techniques for Future Wireless Networks*. Montreal, QC, Canada: École De Technologie Supérieure, 2018.

[19] R. Y. Mesleh, H. Haas, S. Sinanovic, C. W. Ahn, and S. Yun, "Spatial modulation," *IEEE Trans. Veh. Technol.*, vol. 57, no. 4, pp. 2228–2241, Jul. 2008.

[20] P. A. J. Montalban, J. Barrueco, and J. D. Prothero, *Extending the Shannon Upper Bound Using Spiral Modulation*. Leioa, Spain: University of the Basque Country (UPV/EHU), May 2017.

[21] L. Shi, Y.-S. Wang, Y.-W.-P. Hong, and W.-T. Chen, "Coordinated beamforming and power allocation for multicell NOMA systems," in *Proc. IEEE 18th Int. Workshop Signal Process. Adv. Wireless Commun. (SPAWC)*, Jul. 2017, pp. 1–5.

[22] W. Shin, M. Vaezi, B. Lee, D. J. Love, J. Lee, and H. V. Poor, "Non-orthogonal multiple access in multi-cell networks: Theory, performance, and practical challenges," *IEEE Commun. Mag.*, vol. 55, no. 10, pp. 176–183, Oct. 2017.

[23] W. Shin, M. Vaezi, B. Lee, D. J. Love, J. Lee, and H. V. Poor, "Coordinated beamforming for multi-cell MIMO-NOMA," *IEEE Commun. Lett.*, vol. 21, no. 1, pp. 84–87, Jan. 2017.

[24] D. K. Hendraningrat, B. Narottama, and S. Y. Shin, "On the performance of coordinated beamforming based non-orthogonal multiple access in multicell scenarios," in *Proc. Korean Inst. Commun. Sci. Summer Conf.*, vol. 69, no. 1, Jun. 2019, pp. 286–287.

[25] C.-B. Chae, I. Hwang, R. W. Heath, and V. Tarokh, "Interference aware-coordinated beamforming in a multi-cell system," *IEEE Trans. Wireless Commun.*, vol. 11, no. 10, pp. 3692–3703, Oct. 2012.
[26] C. Na, X. Hou, and A. Harada, "Two-cell coordinated transmission scheme based on interference alignment and MU-MIMO beamforming," in *Proc. IEEE 75th Veh. Technol. Conf. (VTC Spring)*, May 2012, pp. 1–5.
[27] F. Kara and H. Kaya, "Spatial multiple access (SMA): Enhancing performances of MIMO-NOMA systems," in *Proc. 42nd Int. Conf. Telecommun. Signal Process. (TSP)*, Jul. 2019, pp. 466–471.
[28] J. W. Kim, M. Irfan, S. M. Al, and S. Y. Shin, "Selective non-orthogonal multiple access (NOMA) and spatial modulation (SM) for improved spectral efficiency," in *Proc. Int. Symp. Intell. Signal Process. Commun. Syst. (ISPACS)*, Nov. 2015, pp. 552–555.
[29] J. W. Kim, S. Y. Shin, and V. C. M. Leung, "Performance enhancement of downlink NOMA by combination with GSSK," *IEEE Wireless Commun. Lett.*, vol. 7, no. 5, pp. 860–863, Oct. 2018.
[30] Q. Li, M. Wen, E. Basar, H. V. Poor, and F. Chen, "Spatial modulation-aided cooperative NOMA: Performance analysis and comparative study," *IEEE J. Sel. Topics Signal Process.*, vol. 13, no. 3, pp. 715–728, Jun. 2019.
[31] C. Zhong, X. Hu, X. Chen, D. W. K. Ng, and Z. Zhang, "Spatial modulation assisted multi-antenna non-orthogonal multiple access," *IEEE Wireless Commun.*, vol. 25, no. 2, pp. 61–67, Apr. 2018.
[32] M. Zeng, A. Yadav, O. A. Dobre, G. I. Tsiropoulos, and H. V. Poor, "Capacity comparison between MIMO-NOMA and MIMO-OMA with multiple users in a cluster," *IEEE J. Sel. Areas Commun.*, vol. 35, no. 10, pp. 2413–2424, Oct. 2017.
[33] Y. Liu, G. Pan, H. Zhang, and M. Song, "On the capacity comparison between MIMO-NOMA and MIMO-OMA," *IEEE Access*, vol. 4, pp. 2123–2129, 2016.
[34] A. A. Tijani, N. Pillay, and H. Xu, "Detection of GSM and GSSK signals with soft-output demodulators," *SAIEE Afr. Res. J.*, vol. 109, no. 1, pp. 15–22, Mar. 2018.
[35] E. Basar, M. Wen, R. Mesleh, M. Di Renzo, Y. Xiao, and H. Haas, "Index modulation techniques for next-generation wireless networks," *IEEE Access*, vol. 5, pp. 16693–16746, 2017.
[36] S. Guo, H. Zhang, P. Zhang, S. Dang, C. Liang, and M.-S. Alouini, "Signal shaping for generalized spatial modulation and generalized quadrature spatial modulation," *IEEE Trans. Wireless Commun.*, vol. 18, no. 8, pp. 4047–4059, Aug. 2019.
[37] A. Younis, N. Serafimovski, R. Mesleh, and H. Haas, "Generalised spatial modulation," in *Proc. Conf. Rec. Forty 4th Asilomar Conf. Signals, Syst. Comput.*, Nov. 2010, pp. 1498–1502.
[38] R. Mesleh, S. S. Ikki, and H. M. Aggoune, "Quadrature spatial modulation," *IEEE Trans. Veh. Technol.*, vol. 64, no. 6, pp. 2738–2742, Jun. 2015.
[39] Z. Yiggit and E. Basar, "Quadrature spatial modulation for large scale MIMO systems," in *Proc. 25th Signal Process. Commun. Appl. Conf. (SIU)*, May 2017, pp. 1–4.
[40] I. Al-Nahhal, O. A. Dobre, E. Basar, and S. Ikki, "Low-cost uplink sparse code multiple access for spatial modulation," *IEEE Trans. Veh. Technol.*, vol. 68, no. 9, pp. 9313–9317, Sep. 2019.
[41] R. F. Siregar, F. W. Murti, and S. Y. Shin, "Bit allocation approach of spatial modulation for multi-user scenario," *J. Netw. Comput. Appl.*, vol. 127, pp. 1–8, Feb. 2019.
[42] M. R. Usman, A. Khan, M. A. Usman, Y. S. Jang, and S. Y. Shin, "On the performance of perfect and imperfect SIC in downlink non orthogonal multiple access (NOMA)," in *Proc. Int. Conf. Smart Green Technol. Electr. Inf. Syst. (ICSGTEIS)*, Oct. 2016, pp. 102–106.
[43] H. SHI, R. V. Prasad, E. Onur, and I. G. M. M. Niemegeers, "Fairness in wireless networks:Issues, measures and challenges," *IEEE Commun. Surveys Tuts.*, vol. 16, no. 1, pp. 5–24, 1st Quart., 2014.
[44] E. Basar, U. Aygolu, E. Panayirci, and H. V. Poor, "Performance of spatial modulation in the presence of channel estimation errors," *IEEE Commun. Lett.*, vol. 16, no. 2, pp. 176–179, Feb. 2012.
[45] J. W. Craig, "A new, simple and exact result for calculating the probability of error for two-dimensional signal constellations," in *Proc. MILCOM Conf. Rec.*, Nov. 1991, pp. 571–575.
[46] G. Sharma, P. K. Sharma, and P. Garg, "Performance analysis of full duplex relaying in multicell environment," in *Proc. Int. Conf. Adv. Comput., Commun. Informat. (ICACCI)*, Sep. 2014, pp. 2501–2505.
[47] N. R. Naidoo, H. J. Xu, and T. A.-M. Quazi, "Spatial modulation: Optimal detector asymptotic performance and multiple-stage detection," *IET Commun.*, vol. 5, no. 10, pp. 1368–1376, Jul. 2011.

DENNY KUSUMA HENDRANINGRAT (Member, IEEE) received the B.Eng. degree in telecommunication engineering from the Telkom Institute of Technology (currently known as Telkom University), Indonesia, in 2011, and the M.Eng. degree from the Department of IT Convergence Engineering, Kumoh National Institute of Technology, South Korea, in 2020. He is currently working with the Deputy for Standards Development, National Standardization Agency of Indonesia. His research interests include wireless communications, frequency management and regulation, and standardization and conformity assessment.

GANDEVA BAYU SATRYA (Senior Member, IEEE) received the bachelor's degree in informatics engineering from STT Telkom, in March 2008, the master's degree in informatics engineering majoring in media informatics from ITTelkom, Bandung, Indonesia, in June 2012, and the Ph.D. degree in security communication in next-generation networks from the Department of IT Convergence Engineering, Kumoh National Institute of Technology, South Korea, in 2019. He is currently a Lecturer and a Researcher with the Faculty of Informatics, Telkom University, Bandung. His research interests include routing protocol, packet scheduling, and security communication in next-generation networks.

I NYOMAN APRAZ RAMATRYANA received the bachelor's degree in telecommunication engineering and the master's degree in electrical and telecommunication engineering from the Telkom Institute of Technology (currently known as Telkom University), Indonesia, in 2010 and 2014, respectively. He is currently pursuing the Ph.D. degree in IT convergence engineering with the Kumoh National Institute of Technology, South Korea. His research interests include signal processing, machine learning, computer vision, polar coding, raptor coding, non-orthogonal multiple access (NOMA), and multiple-input multiple-output (MIMO) antenna.